ELSEVIER

International Journal of Mass Spectrometry 185/186/187 (1999) 165–177

International Journal of Mass Spectrometry

Ethene loss kinetics of methyl butanoate ions studied by threshold photoelectron–photoion coincidence: the enol ion of methyl acetate heat of formation

Oleg A. Mazyar, Tomas Baer*

Chemistry Department, The University of North Carolina at Chapel Hill, Chapel Hill, NC 27599-3290, USA

Received 20 May 1998; accepted 28 July 1998

Abstract

Threshold photoelectron–photoion coincidence spectroscopy has been used to investigate the unimolecular chemistry of gas-phase methyl butanoate ions ($CH_3CH_2CH_2COOCH_3^{\cdot+}$). This ester ion isomerizes to a lower energy distonic ion ($CH_2CH_2CH_2COHOCH_3^{\cdot+}$) prior to dissociating by the loss of C_2H_4. The asymmetric time of flight distributions, which arise from the slow rate of dissociation at low ion energies, provide information about the ion dissociation rates. By modeling these rates with assumed $k(E)$ functions, the thermal energy distribution for room temperature and molecular beam samples, and the analyzer function for threshold electrons, it was possible to extract the dissociative photoionization limit for methyl butanoate which at 0 K is 10.275 ± 0.010 eV as well as the dissociation barrier of the distonic ion of 0.735 ± 0.010 eV. By combining these with an estimated heat of formation of methyl butanoate, we derive a 0 K heat of formation of the distonic ion $CH_2CH_2CH_2COHOCH_3^{\cdot+}$ of 119.0 ± 2.0 kcal/mol. The product ion is the enol of methyl acetate, $CH_2COHOCH_3^{\cdot+}$, which has a derived heat of formation at 0 K of 122.0 ± 2.0 kcal/mol. This energy agrees well with a derived energy obtained recently from the rate analysis of energy selected methyl acetate ions. Also measured was the adiabatic ionization energy of the methyl butanoate, 9.95 ± 0.05 eV. (Int J Mass Spectrom 185/186/187 (1999) 165–177) © 1999 Elsevier Science B.V.

Keywords: Kinetic energy release; Keto–enol tautomerization; Ionization energy

1. Introduction

The dissociation dynamics of gas phase ester ions, R′ COOR, are very complex. Most of these ions rearrange to more stable ions prior to dissociation. Among the list of eclectic neutral fragments lost by various ester ions are H_2O, alkenes, CO, H atoms, and RO· radicals [1–3]. It is apparent that most of the neutral fragments are closed shell molecules and that all, except for the RO· radical loss channel, must involve rearrangements prior to dissociation. Two reasons for this complexity of these reactions are the low barriers for isomerization and the variety of low energy isomers produced in the rearrangement process. These isomers involve transfer of hydrogen atoms from various locations on the R′ and R groups to one of the two oxygen atoms, thereby creating a variety of distonic (charge and radical sites on separate atoms) and enol structures.

We have investigated the dissociation rates for a

* Corresponding author.

Dedicated to Professor Michael T. Bowers on the occasion of his 60th birthday.

PII S1387-3806(98)14146-5

number of the ester ions and have found that several of them dissociate via two-component dissociation rates [1,2,4]. Such two component processes arise when isomerization and dissociation are in competition. A general mechanism can be written as follows:

$$A^+ + B \xleftarrow{k_1} AB^+ \underset{k_3}{\overset{k_2}{\rightleftarrows}} CD^+ \quad (1)$$

where CD^+ is a low energy isomer of AB^+. If $k_2 \gg k_1$, all ions rearrange to the CD^+ structure prior to dissociation, and thus, dissociate with a slow rate constant determined by the depth of the potential well of CD^+. If, however, $k_1 \gg k_2$, then none of the ions isomerize and the rate will be fast. Now if $k_1 \approx k_2$, then some ions dissociate rapidly by direct dissociation to $A^+ + B$, while some isomerize and come back much more slowly. This situation gives rise to two-component dissociation. Whether this is observed or not depends very sensitively on the relative barrier heights for direct dissociation (via k_1) and isomerization (via k_2).

In the case of the methyl acetate ion dissociation, ab initio molecular orbital (MO) calculations showed that at least two isomers participated in the reaction dynamics [4,5]. Tautomerization of the parent ion to its enol form, $CH_2COHOCH_3^+$, proceeds via two consecutive [1,4] hydrogen shifts with a distonic ion intermediate, $CH_3COHOCH_2^+$. The lower energy enol form is the one that ultimately determines the slow component of the rate constant. Since no accurate experimental value of this ion structure was known, we used its energy as an adjustable parameter in order to fit the rate versus energy curve for the methyl acetate ion dissociation [4]. This lead to a 0 K enol ion heat of formation of 123 ± 3 kcal/mol. Because this energy was one of several parameters that was adjusted and because its assumed energy depended on the choice of activation entropy, a critical test of the proposed methyl acetate ion model involves the comparison of the assumed heat of formation for the enol ion with a good experimental value. This is, in part, the purpose of the present paper.

The methyl butanoate ions dissociate exclusively by the loss of ethylene, and yield the enol ion of methyl acetate [3,6]. They do this by prior isomerization to a distonic ion, $CH_2CH_2CH_2COHOCH_3^+$. It is evident that the loss of the terminal CH_2CH_2 group results in the aforementioned enol ion of methyl acetate. Because the methyl butanoate distonic ion can form the enol ion of methyl acetate via a simple bond break, it will do so without a reverse activation barrier. Thus, a measure of the onset for ethylene loss from methyl butanoate ion should yield a good value for the methyl acetate enol ion heat of formation.

2. Experimental approach

The experimental apparatus has been previously described [7]. Briefly, sample molecules were ionized with vacuum ultraviolet light from a H_2 discharge lamp dispersed by a 1 m normal incidence monochromator. An electric field of 20 V/cm accelerates electrons and ions in opposite directions. Threshold electrons were selected by a steradiancy [8,9] and hemispherical analyzers (~30 meV combined photon and electron energy resolution) and detected with an electron multiplier. The resulting ions were detected in coincidence with their corresponding electrons. The time difference between the two detection events defines the ion's time-of-flight (TOF). For each coincidence event, the TOF was electronically converted to a peak height and sorted on a multichannel analyzer. TOF distributions were obtained in 10–12 h.

For thermal samples, room temperature vapor was leaked into the experimental chamber through a needle valve. In the molecular beam experiments, the translationally and internally cooled sample was generated by continuous expansion through a 50 μm nozzle of a 10% mixture of methyl butanoate in argon at a total backing pressure of 290 Torr.

Two experiments were performed. The fractional abundance of product and parent ions were measured as a function of the photon energy. The dissociative photoionization onset, DP_0, was derived from this breakdown diagram. The related experiment involved measuring the product ion TOF distributions. Slowly dissociating ions decay as they are accelerating in the

5 cm long acceleration region. This results in asymmetric TOF distributions from which a dissociation rate can be extracted. The breakdown diagram and the ion TOF distributions are related and must be analyzed as a single data set.

3. Ab initio molecular orbital calculations

The comparison of the experimental dissociation rates of methyl butanoate ions with predictions of the statistical Rice–Ramsperger–Kassel–Marcus (RRKM) theory (to be discussed later), demonstrates that these ions must rearrange to a lower energy structure prior to dissociating. In the absence of isomerization, the difference between the ionization energy of 10.07 eV [10] and the measured dissociation onset of 10.17 eV [6] implies an activation energy of only 0.1 eV. Such a small activation energy would result in a dissociation rate constant in excess of 10^{11} s^{-1}. Because the minimum observed dissociation rate constant is less than 10^5 s^{-1}, an isomerization to a lower energy structure is clearly required if these dissociation rates are to be consistent with predictions of the statistical theory. In order to discuss the data analysis more meaningfully, we present first the results of the ab initio MO calculations which provide us with the identity of the isomeric structure and an estimate of its energy.

The dissociation of metastable methyl butanoate ions (see structure A in Fig. 1) was used by Schwarz et al. [11] and Holmes et al. [3,6] as a source of the enol isomer of the methyl acetate ion (structure F in Fig. 1). It was suggested that the $CH_2COHOCH_3^{\cdot+}$ ion was formed as a result of a simple ethene loss reaction of the distonic isomer of methyl butanoate ion, B, which, in turn, is a product of [1,5]-methyl hydrogen transfer to the carbonyl oxygen in methyl butanoate [11]. Isomerization reaction pathways and possible involvement of other isomers of methyl butanoate ion in the isomerization/dissociation mechanism of ionized methyl butanoate have not been studied. It is known, however, that ionized esters may undergo multiple rearrangement processes before the dissociation step itself, which are often in competition with each other as well as with the dissociation channel [4,5,12].

In order to elucidate the isomerization/dissociation mechanism of the ionized methyl butanoate, ab initio MO calculations have been carried out with the GAUSSIAN-94 series of programs [13]. Five stable $C_5H_{10}O_2^{\cdot+}$ radical-cation structures and five transition states linking them were found (see Fig. 1 and Table 1). Their vibrational frequencies and zero-point vibrational energies (ZPE) were calculated at the unrestricted Hartree–Fock level of theory using the split-valence 6-31g* basis set, which includes a set of polarization functions for all nonhydrogen atoms. Harmonic vibrational frequencies and ZPEs were corrected by factors 0.8929 and 0.9135, respectively, to take into account the fact that at the UHF/6-31g* level the fundamental frequencies are overestimated by ~10% [14,15] (see Tables 1 and 2). Transition states between the stable isomers were proved by using the intrinsic reaction coordinate method at the UHF/6-31g* level of theory [13].

To further improve the reliability of calculations, electron correlation was included by using second-order Møller–Plesset perturbation theory (MP2). Geometries of $C_5H_{10}O_2^{\cdot+}$ structures optimized at the MP2(FULL)/6-31g* level of theory are shown in the Fig. 1. Bond lengths are given in angstroms and bond angles in degrees. Energies for these structures are listed in Table 1. The spin contaminations, $\langle S^2 \rangle$, were within an acceptable range and close to the value of 0.76 for most of the stable isomers and transition states (see Table 1). However, $\langle S^2 \rangle$ values were found to be slightly higher (close to 0.79) for the transition states TSAC, TSBC, and TSCD. Table 1 also shows the relative energies of all structures with respect to the energy of the methyl butanoate ion (isomer A in Fig. 1) calculated at the MP2(FULL)/6-31g* + ZPE level of theory.

The relative energy of the transition state TSAB (see Fig. 1) connecting methyl butanoate ion A to its distonic isomer $CH_2CH_2CH_2COHOCH_3^{\cdot+}$ (structure B in Fig. 1) by means of a [1,5]-methyl hydrogen shift to the carbonyl oxygen was found to be only 0.81 kcal/mol. This isomerization barrier is significantly lower than the barrier of 15.3 kcal/mol for the

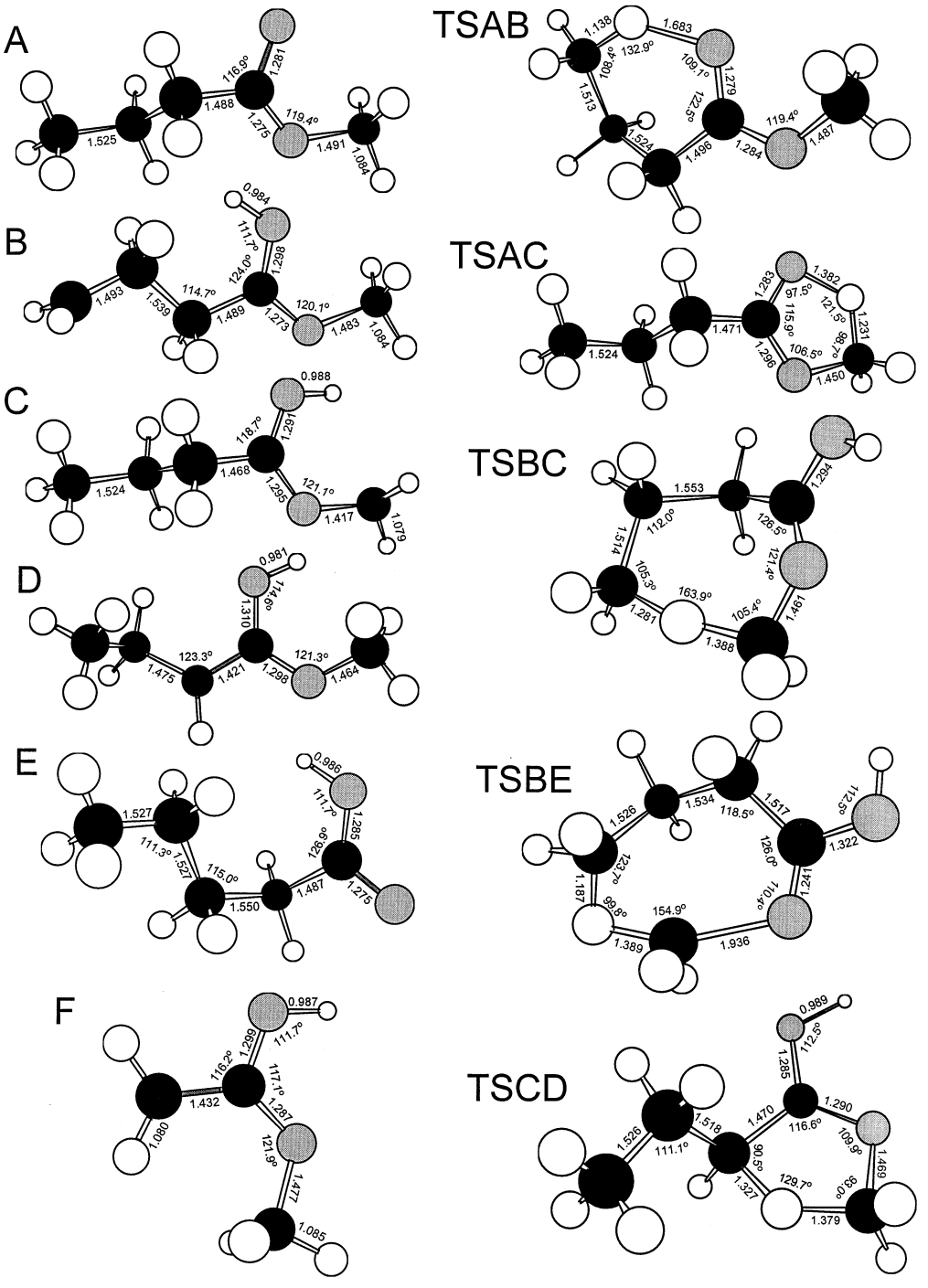

Fig. 1. MP2(FULL)/6-31g* optimized geometries of the various isomers of the methyl butanoate ion and the transition states linking them.

Table 1
Calculated energies and ZPE of ions, transition states, and dissociation products

	ZPE[a]/HF/6-31g*, (hartrees)	MP2(FULL)/6-31g*, (hartrees)	E_{rel}, MP2(FULL)/6-31g*, (kcal/mol)	$\langle S^2 \rangle$ MP2(FULL)/6-31g*
Species				
A	0.156 750	−345.571 296 7	0.0	0.761
B	0.155 203	−345.594 766 0	−15.614	0.763
C	0.156 036	−345.587 067 2	−10.305	0.759
D	0.157 173	−345.609 424 8	−23.683	0.760
E	0.157 743	−345.567 795 0	2.767	0.761
TSAB	0.152 204	−345.565 854 8	0.809	0.766
TSAC	0.151 898	−345.542 526 5	15.272	0.786
TSBC	0.152 457	−345.557 921 4	5.932	0.787
TSBE	0.150 966	−345.490 136 7	47.613	0.766
TSCD	0.151 740	−345.547 371 9	12.141	0.794
Products				
F	0.096 123	−267.254 181 6		0.760
$CH_2{=}CH_2$	0.054 772	−78.294 286 2		
Products			10.969	

[a] To be scaled by 0.9135 [14,15].

[1,4]-methoxy hydrogen transfer to the carbonyl oxygen, which leads to the formation of the second distonic ion $CH_3CH_2CH_2COHOCH_2^+$ (structure C). This is consistent with findings of Yates et al. [16], who noted that [1,5]-H transfers require less energy that [1,4]-H shifts. Although the barrier between isomers A and C is higher than the dissociation limit, isomer C can be accessed via a much lower barrier from isomer B. The energy of this [1,6]-H atom transfer transition state (TSBC) was found to be 5 kcal/mol below the dissociation limit. This implies that isomer C does, in fact, participate in the isomerization/dissociation reaction of methyl butanoate ion.

The distonic isomer C is linked with the enol isomer of methyl butanoate ion, D, via the transition state TSCD. This rearrangement requires 12.1 kcal/mol, which is only 1.2 kcal/mol higher than the energy of reaction products (see Table 1). Thus, we cannot rule out the participation of enol structure D in the isomerization/dissociation reaction of methyl butanoate ion on the basis of theoretical calculations. But, the involvement of isomer D can be excluded on the basis of the RRKM simulations of the threshold photoelectron–photoion coincidence (TPEPICO) TOF spectra. Because it lies some 8 kcal/mol below the lowest energy distonic isomer B, the dissociation rates would be much lower than actually measured.

In the course of our search for the transition state linking two distonic isomers, B and C, the transition state TSBE connecting isomer B with ionized pentanoic acid, E, was found. In this transition state (see Fig. 1) one of the methoxy hydrogens forms a bond with the methylene carbon in the isomer B and then drags the rest of the methoxy group to this carbon. The modulus of the imaginary frequency for this transition state is 649 cm^{-1}. The barrier for the rearrangement of the distonic ion of the methyl butanoate, B, to the pentanoic acid E was found to be 47.6 kcal/mol, which excludes it from participation.

On the basis of these calculations and the experimental results to be described, it appears that only two distonic isomers, B and C, participate in the low energy dissociation mechanism of methyl butanoate ions. Because the energy of the transition state TSBC linking these two structures is considerably lower than the energy of the reaction products, the two distonic ions must be in rapid equilibrium with each other. That is, the rates for interconversion among the distonic isomers are much faster than the rate of dissociation of isomer B. This implies that in terms of the potential energy surface of the isomerization/dissociation reaction of methyl butanoate ion, the distonic ion isomers B and C can be treated as a single well [17]. However, we need to take into account their

Table 2
Vibrational harmonic frequencies used in this study[a]/cm^{-1}

A (neutral)	43, 80, 142, 146, 171, 233, 296, 324, 416, 568, 686, 726, 865, 870, 884, 997, 1014, 1100, 1106, 1159, 1191, 1222, 1227, 1294, 1319, 1396, 1407, 1439, 1459, 1461, 1467, 1469, 1473, 1477, 1795, 2855, 2870, 2883, 2893, 2900, 2902, 2918, 2926, 2974, 2989
A	15, 80, 105, 127, 190, 231, 252, 305, 373, 544, 615, 721, 814, 842, 856, 903, 986, 1081, 1102, 1138, 1172, 1220, 1264, 1297, 1344, 1366, 1403, 1407, 1426, 1441, 1457, 1459, 1465, 1473, 1570, 2867, 2874, 2881, 2913, 2929, 2936, 2945, 2953, 3029, 3064
B	26, 84, 99, 125, 146, 181, 274, 310, 375, 418, 540, 633, 634, 731, 840, 852, 882, 988, 1017, 1102, 1143, 1146, 1199, 1230, 1259, 1298, 1353, 1398, 1422, 1427, 1446, 1458, 1469, 1473, 1628, 2845, 2882, 2888, 2929, 2938, 2983, 3038, 3061, 3086, 3575
C	37, 76, 95, 120, 224, 234, 266, 305, 397, 577, 631, 725, 729, 774, 844, 865, 872, 973, 984, 1074, 1109, 1120, 1182, 1219, 1270, 1290, 1347, 1393, 1404, 1439, 1460, 1463, 1473, 1501, 1566, 2875, 2882, 2916, 2917, 2941, 2950, 2976, 2990, 3137, 3534
D	18, 82, 148, 165, 171, 236, 290, 325, 424, 492, 594, 623, 712, 759, 861, 866, 948, 1025, 1043, 1121, 1140, 1142, 1186, 1243, 1277, 1367, 1401, 1418, 1444, 1452, 1464, 1467, 1471, 1506, 1575, 2850, 2878, 2908, 2931, 2946, 2956, 2997, 3035, 3047, 3598
E	30, 76, 106, 192, 233, 242, 363, 415, 497, 585, 689, 726, 786, 794, 874, 912, 925, 1002, 1077, 1092, 1132, 1177, 1228, 1284, 1306, 1309, 1372, 1405, 1417, 1450, 1457, 1461, 1465, 1479, 1580, 2837, 2865, 2875, 2894, 2896, 2935, 2942, 2948, 2954, 3543
TSAB	2033i, 86, 121, 178, 204, 226, 363, 422, 434, 499, 577, 692, 819, 845, 855, 879, 905, 1004, 1095, 1126, 1144, 1179, 1187, 1220, 1266, 1318, 1344, 1378, 1412, 1423, 1438, 1446, 1451, 1458, 1459, 1578, 2874, 2895, 2928, 2933, 2938, 2963, 3006, 3030, 3058
TSAC	2573i, 34, 77, 113, 234, 238, 302, 346, 416, 602, 641, 724, 748, 852, 863, 944, 972, 987, 1073, 1084, 1107, 1131, 1142, 1213, 1266, 1290, 1345, 1393, 1404, 1428, 1460, 1462, 1463, 1472, 1511, 1682, 2876, 2884, 2909, 2919, 2942, 2951, 2970, 2975, 3090
TSBC	2195i, 72, 181, 191, 275, 324, 346, 449, 501, 531, 633, 660, 715, 745, 832, 858, 899, 962, 996, 1073, 1094, 1138, 1157, 1198, 1231, 1232, 1321, 1339, 1354, 1394, 1409, 1426, 1444, 1462, 1518, 1578, 2891, 2896, 2926, 2934, 2976, 2976, 3004, 3086, 3525
TSBE	649i, 57, 85, 185, 202, 252, 285, 332, 368, 433, 484, 556, 629, 710, 768, 861, 871, 917, 948, 1009, 1035, 1078, 1163, 1175, 1216, 1282, 1303, 1311, 1381, 1414, 1423, 1433, 1442, 1516, 1730, 1987, 2869, 2889, 2915, 2922, 2932, 2991, 3001, 3166, 3644
TSCD	2348i, 71, 79, 158, 206, 237, 298, 433, 465, 555, 606, 639, 705, 745, 841, 872, 901, 952, 1000, 1072, 1081, 1109, 1129, 1200, 1231, 1271, 1306, 1350, 1398, 1405, 1453, 1463, 1466, 1512, 1555, 1628, 2871, 2876, 2905, 2938, 2943, 2953, 2986, 3099, 3508
F	146, 163, 262, 302, 445, 514, 575, 660, 748, 807, 987, 997, 1141, 1158, 1215, 1399, 1429, 1452, 1464, 1527, 1587, 2930, 3017, 3029, 3056, 3132, 3532
$CH_2{=}CH_2$	801, 978, 982, 1031, 1208, 1337, 1438, 1657, 2965, 2986, 3031, 3054

[a] Scaled by 0.8929 HF/6-31g* frequencies [14]. Transition state imaginary frequencies denoted (i).

contribution to the total density of states. This is done in the following manner [17]. Suppose the isomers B and C have energies (relative to the methyl butanoate ion) of E_B and E_C. The total density of states at the energy E (again relative to the methyl butanoate ion) will be given by

$$\rho(E) = \rho(E - E_B) + \rho(E - E_C) \quad (2)$$

Taking into account the fact that the low-frequency modes of isomers B and C are very close (see Table 2), it is clear that the deepest well, namely the one corresponding to distonic ion B, contributes the most to the total density of states. Moreover, these two isomers are calculated to differ by as much as 5.3 kcal/mol in energy. As a result, the contribution of isomer B to the total density of states is significantly

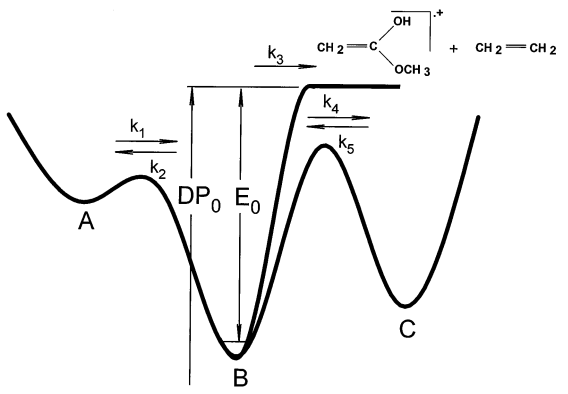

Fig. 2. Two-well–one-product potential energy surface for the dissociation/isomerization of the ionized methyl butanoate (approximately to scale).

higher than that of isomer C. Thus, isomer C does not affect the rate of reaction. However, it does participate in hydrogen scrambling. The three-well model in Fig. 2 predicts that the six terminal hydrogens are scrambled, while the remaining four hydrogens are not. This prediction could be readily tested by studies with isotopically labeled species.

It has been our experience that the energies obtained by ab initio MO calculations are not sufficiently precise to permit their use without some adjustment in modeling the statistical theory fit to the experimental rate constants. We thus use the present calculations as a starting point and permit adjustments of ± 5 kcal/mol. On the other hand, we choose to use the vibrational frequencies of the stable structures A and B and the transition state TSAB as given by the ab initio MO calculations. Because structure C does not affect the dynamics, it is ignored in the analysis of the rates.

All indications are that the barrier for isomerization from the methyl butanoate ion is very low. In addition, there is no low energy direct path through which the methyl butanoate ion can dissociate without first isomerizing. Thus, we do not expect that this ion will dissociate via a two-component rate constant. This distinguishes this ion from methyl acetate, methyl formate, and ethyl formate, all of which dissociate via two-component mechanisms [1,2,4].

4. Experimental results

4.1. TOF distributions and breakdown diagrams

TOF mass spectra of methyl butanoate were collected over the photon energy range 10.15–10.80 eV. Typical TOF distributions of ionized methyl butanoate are shown in Figs. 3 and 4. Parent ion peaks in the molecular beam data are narrower (~40 ns) in comparison with the room temperature data, because of cooling of translational degrees of freedom orthogonal to the beam axis down to as low as 10 K during the supersonic expansion. One can also see a significant difference in the relative area and the shape of the fragment ion peaks in the molecular beam and 298 K spectra collected at the same photon energy of 10.35 eV. The fragment ion peak is less intense in the molecular beam data because the free jet expansion has removed some of the internal energy, thus lowering the dissociation rate constant. Because of the lower energy and the narrower TOF peaks, the fragment ion peak in the molecular beam TOF mass spectrum is more asymmetric.

Fig. 5 shows the breakdown diagrams which consist of the fractional abundance of parent and daughter ions. The parent ion signal was obtained by integrat-

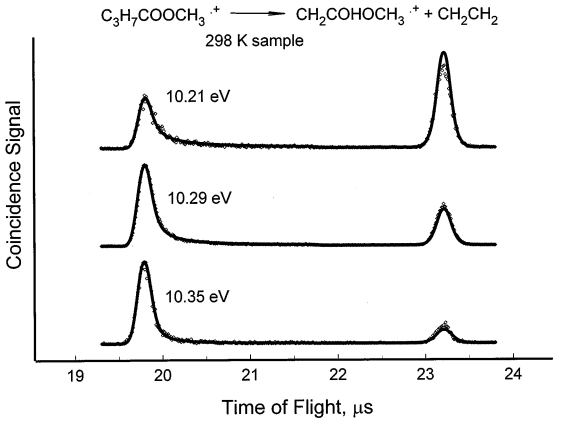

Fig. 3. Coincidence mass spectra (diamonds) of the 298 K sample of methyl butanoate at three photon energies. The solid line is a calculated TOF distribution modeled by application of the internal energy distribution function in Fig. 6 to the dissociation rate curve shown in Fig. 7.

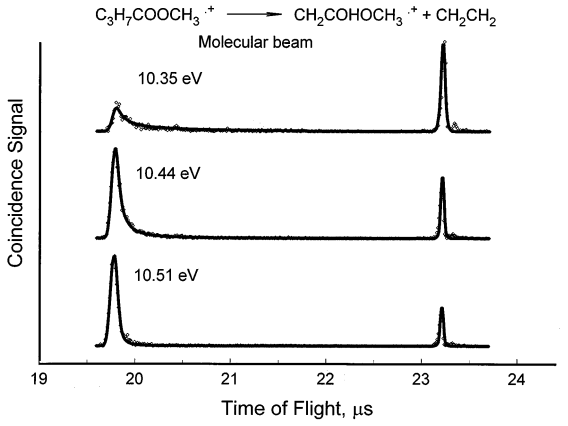

Fig. 4. Coincidence mass spectra (diamonds) of the molecular beam sample of methyl butanoate at three photon energies. The solid line is a calculated TOF distribution modeled by application of the internal energy distribution function in Fig. 6 to the dissociation rate curve shown in Fig. 7.

ing the signal between 22.9 and 23.5 μs (Figs. 3 and 4), while the daughter ion peaks were obtained by integration of the signal between 19.5 and 21.8 μs. Some of the parent ion signal contains low energy ions with energy in excess of the dissociation limit, but which have not decayed in the acceleration region. Cooling of the internal degrees of freedom of the methyl butanoate molecules during the adiabatic gas dynamic expansion is most clearly evident in the shift of the crossover energy [7]. It is interesting that a significant fragment ion peak (relative abundance of about 30%) appears at the lowest photon energy investigated which is just slightly in excess of the ionization energy (IE) of the methyl butanoate. This is a result of the broad thermal energy distribution and the small energy difference between the ionization and dissociation limits.

According to the ab initio MO calculations, the dissociation dynamics of metastable methyl butanoate ions can be described by a single rate constant, k_3 (see Fig. 2). In other words, in the case of perfectly energy selected molecular ions, fragment ion TOF distributions would be the single component. However, detailed analysis of our TOF distributions shows that the data must be interpreted in terms of a distribution of rate constants. The multicomponent dissociation kinetics are observed because the broad molecular ion internal energy distribution in our experiment leads to a broad distribution of dissociation rate constants, $k_3(E)$. This problem is particularly severe in the case of methyl butanoate because the average vibrational and rotational energy is 202 meV at room temperature, and the distribution is spread over 500 meV. As will be shown, the rate constant, $k_3(E)$, varies over several orders of magnitude in this energy range.

4.2. Data analysis

The extraction of an activation energy, E_0 (see Fig. 2), from the breakdown diagram and TOF distributions requires careful treatment of the dissociation rate constant, $k_3(E)$, the thermal energy distribution of the sample molecules, and the energy resolution function of our threshold electron analyzer. As shown by Keister et al. [18] when these are properly taken into account both the breakdown diagram and the TOF distributions can be fitted.

The first step in the analysis is the calculation of the thermal energy distribution of methyl butanoate molecules using a Boltzmann formula

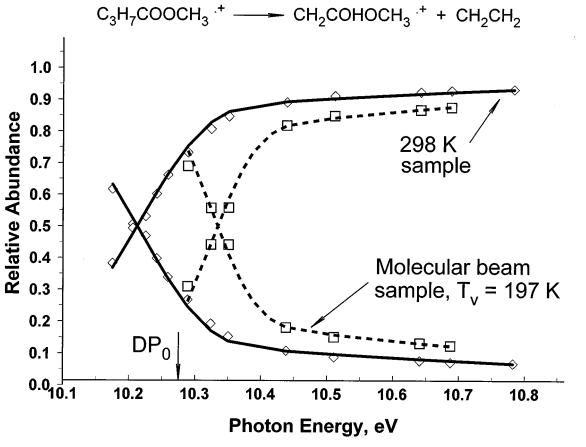

Fig. 5. Breakdown diagrams for 298 and 141 K internal energy distributions. The points are the experimental data, while lines are calculated by taking into account the internal energy distribution of ionized methyl butanoate and the microcanonical dissociation rate constant $k_3(E)$ shown in Fig. 7. The energy corresponding to DP_0 is the 0 K dissociative photoionization threshold.

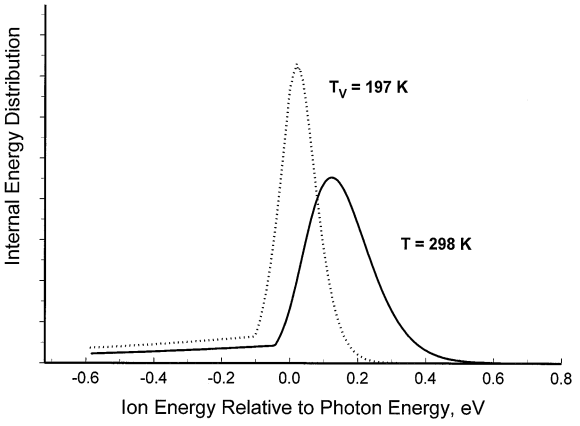

Fig. 6. Ion rovibrational energy distributions for 298 K sample (solid line) and molecular beam sample (dotted line), obtained by convolution of the sample thermal vibrational energy distribution with the electron energy analyzer function. Zero on the abscissa corresponds to the photon energy.

$$P(E_{\text{th}}) = \frac{\rho(E_{\text{th}})\ e^{-E_{\text{th}}/kT}}{\int_0^\infty \rho(E_{\text{th}})\ e^{-E_{\text{th}}/kT}\, dE_{\text{th}}} \tag{3}$$

where the rovibrational density of states $\rho(E_{\text{th}})$ is calculated using an exact count algorithm [17]. The methyl butanoate molecule was approximated with a symmetric top, whose moment of inertia I_{C} was taken directly from the ab initio MO calculations, $I_{\text{C}} = 8.57$ GHz, while the two other, I_{A} and I_{B}, were calculated as an average geometric of the ab initio values, 1.20 and 1.08 GHz.

The distribution of ion internal thermal energy is represented by a convolution of the electron energy analyzer function with the thermal energy distribution of methyl butanoate molecules [Eq. 3]. The analyzer function can be measured directly from a threshold photoelectron spectrum of a rare gas, NO, or acetylene (the latter two have widely spaced vibrational levels). Since we do not know the temperature of the molecular beam sample, we begin with the room temperature sample. The result of this convolution is shown in Fig. 6; zero energy in Fig. 6 corresponds to the photon energy. Ion energies below this arise because our electron analyzer permits some energetic electrons to reach the detector. The ion energy is given by

$$E_{\text{ion}} = h\nu - \text{IE} + E_{\text{th}} - E_{\text{el}} \tag{4}$$

where E_{th} is the prior rovibrational energy and E_{el} is the kinetic energy of the ejected electron. Thus the detection of energetic (or "hot") electrons gives rise to lower energy ions. Ion energies above zero in Fig. 6 are due to the broad thermal distribution of molecules. Methyl butanoate, with its 45 vibrational modes, has an average rovibrational energy at 298 K of 202 meV. This drops to 101 meV in the molecular beam sample which we estimate to have a temperature of 197 K (we assume that the molecules in the beam are rotationally cold).

With the energy deposition function of Fig. 6 in hand, the ion TOF distribution over the whole TOF rate from 19.5 to 23.5 μs can be calculated. In this analysis, we take into account the fact that some ions with energy just slightly in excess of the dissociation limit, do not dissociate in the acceleration region because of the small rate constant close to threshold. Ions which decay in the drift region have the same TOF as parent ions and are thus counted as parent ions. Thus, any ion which lives longer than 7.4 μs, the time required for an ion to reach the drift region, is counted as a parent ion. Thus, the "parent ion" peaks in Figs. 3 and 4 consist of ions which have $E < E_0$, and those slowly dissociating ions with $E = E_0 + \delta E$.

The fraction of ions which decay after leaving the acceleration region can be determined quite accurately because modeling of the asymmetric TOF distribution in the region between 19.5 and 21.8 μs of Figs. 3 and 4, with an assumed or calculated $k_3(E)$ function can be used to determine this fraction. The decay rate function, $k_3(E)$ is calculated by RRKM theory [17,19,20]

$$k_3(E) = \frac{\sigma N^{\ddagger}(E - E_0)}{h\rho(E)} \tag{5}$$

where $N^{\ddagger}(E - E_0)$ is the sum of states of the transition state from 0 to $E - E_0$, $\rho(E)$ is the density of states as measured from the bottom of the distonic ion

B well (see Fig. 2), and σ is the reaction degeneracy, which in this case is 1. The activation energy, E_0, is also measured from the bottom of the isomer B energy well. The vibrational frequencies for the density of states calculation are obtained from the ab initio MO calculations. However, the transition state frequencies were estimated. According to the ab initio MO calculations; the loss of ethylene from the distonic isomer of methyl butanoate ion proceeds without a barrier so that the variational transition state theory (VTST) [17,21,22] should be used. However, given the amount of averaging needed to analyze the data, and given the fact that the rates are slow only over a very small energy region above threshold, we chose not to use VTST here. Rather, we simply used the isomer B frequencies except the one of $\sim$1100 cm^{-1} associated with C–C stretch mode, which becomes the imaginary frequency in this transition state, and varied the five lowest ones in order to fit the experimental data. The best fit was when the five lowest frequencies were multiplied by the factor 0.68. These are the frequencies which turn into product rotations and thus are reduced to zero as the ion proceeds toward products.

Two energies needed to be adjusted, the 0 K dissociative photoionization threshold for the ethylene loss, DP_0, and the activation energy of the C_2H_4 loss reaction, E_0, measured from the bottom of the distonic ion B well (see Fig. 2). The breakdown diagram crossover energy (corresponding to 50% of fragment ion fractional abundance) is especially sensitive to the assumed value of DP_0, while the shape of product ion TOF peaks is determined by the dissociation rate, or in other words, by the depth of the distonic ion B well, E_0.

The adjustment of DP_0, E_0, and the transition state frequencies yielded the best fit for the 298 K data shown by the solid lines in Figs. 3 and 5. Variation of the energies by 1 kcal/mol resulted in significantly worse fits to the data. The fit to the data of Figs. 3 and 5 was made using the RRKM theory $k_3(E)$ curve shown in Fig. 7. The minimum rate was found to be about 10^2 s^{-1}. However, it rises rapidly near threshold and reaches a value of 10^5 within 75 meV. This means that the majority of ions with energy between E_0 and E_0 + 75 meV will be collected as parent ions. This

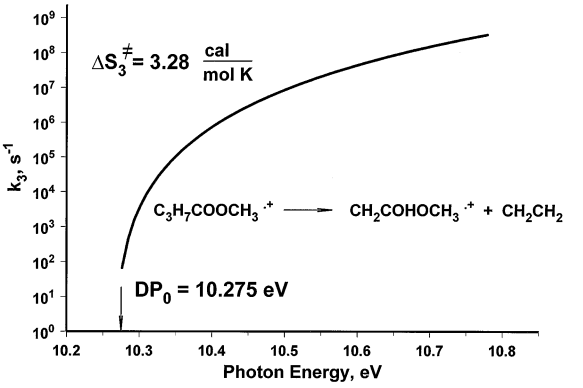

Fig. 7. Experimentally derived microcanonical rate constant for ethylene loss reaction of ionized methyl butanoate.

represents the so-called "kinetic shift" [23,24] which shifts the observed onset to energies above the true DP_0. The analysis described here, takes this into account.

The best fit for the data was provided with an entropy of activation $\Delta S^{\ddagger}_{600K}$ of 3.28 kcal/mol^{-1} K^{-1}. This is calculated in the usual manner [17] from the vibrational frequencies of the molecular ion (the distonic isomer B) and the transition state. As one would expect, this reaction proceeding by a "loose" transition state has a positive activation entropy.

Once the thermal data were analyzed, the molecular beam TOF data and breakdown diagram were fitted by varying only a single parameter, the temperature of the internal degrees of freedom of methyl butanoate in the molecular beam. The excellent fit provides a useful and essential test of the fitting procedure.

The location of the 0 K dissociative photoionization limit, DP_0, relative to the observed crossover energy in the breakdown diagram requires some comments. Three effects shift the observed crossover energy from the ideal 0 K onset. These are the thermal energy distribution, the slow dissociation rate at low energies, and the effect of the "hot electrons". The thermal energy distribution shifts the onset to lower energies, while the other two effects shift it to higher energies. Thus they compensate each other. In the case of the 298 K data, the influence of wide thermal energy distribution is dominant, and the onset falls

Table 3
Experimental energies of relevant species

Species	$\Delta H_{f(0\ K)}$ (neutral), (kcal/mol)	$\Delta H_{f(0\ K)}$ (ion) (kcal/mol)	IE/DP (eV)
$CH_3CH_2CH_2COOCH_3$	-101 ± 2[a]	129 ± 1[b]	9.95 ± 0.05[b]
		131.5[c]	10.07 ± 0.03 [10]
$CH_2CH_2CH_2COHOCH_3$		119 ± 2[b]	
$CH_2COHOCH_3$		122 ± 2[b]	10.275 ± 0.010[b]
		123 ± 3 [4]	10.17 ± 0.05 [3,6]
		118.5 ± 1.0[d]	

[a] The 0 K heat of formation of methyl butanoate was determined by converting the literature value at 298 K of −108.0 kcal/mol [3,6] using the HF/6-31g* vibrational frequencies.
[b] Measured in the present work.
[c] The 0 K heat of formation of methyl butanoate ion was determined by converting the literature value at 298 K of 124.0 kcal/mol [25] using the UHF/6-31g* vibrational frequencies.
[d] The 0 K heat of formation of the enol ion of methyl acetate was determined by converting the literature value at 298 K of 114.0 kcal/mol [3,6] using the UHF/6-31g* vibrational frequencies.

nearly 60 meV below the 0 K threshold. On the other hand, in the molecular beam data with its much narrower thermal energy distribution, the onset is shifted toward higher energies by ~60 meV. In this case, the slow rate constant gives a shift of about +75 meV, while the "hot electron" effect shifts it another 86 meV. This total shift of 161 meV to higher energies is shifted to lower energy by the average thermal energy (101 meV) of the methyl butanoate molecules in the molecular beam.

4.3. The derived thermochemical data

As shown in Table 3, the 0 K dissociative photoionization limit for the $CH_2COHOCH_3^{\cdot+}$ ion plus ethylene products, DP_0, is 10.275 ± 0.010 eV. If we combine this with the 298 K heat of formation of the neutral methyl butanoate of −108 kcal/mol [3,6] ($\Delta H^\circ_{f(0\ K)} = -101$ kcal/mol) and the 0 K heat of formation of ethylene of 14.5 kcal/mol [25], we obtain a 0 K heat of formation of the enol ion of methyl acetate (structure F in Fig. 1) of 122 kcal/mol. The dissociation reaction activation energy, E_0, of 0.735 ± 0.010 eV combined with DP_0 and $\Delta H^\circ_{f(0\ K)}$ [$CH_3CH_2CH_2COOCH_3$] values yields a 0 K heat of formation of the distonic ion $CH_2CH_2CH_2COHOCH_3^{\cdot+}$ of 119 kcal/mol. Unfortunately, the methyl butanoate heat of formation is not an experimental value. Rather it is one calculated by Holmes and Lossing [3] using simple additivity principles so that it is difficult to assign an uncertainty to this value. We arbitrarily assign an uncertainty of ±2 kcal/mol. We calculated the heat of formation of the neutral methyl butanoate using molecular mechanics program (MMX) [26] which gave a value of −105 kcal/mol, which agrees within the combined errors of the MMX and the Holmes estimation. However, it is interesting that modeling of the TPEPICO data on the methyl acetate ion dissociation lead to an enol heat of formation of 123 ± 3 kcal/mol [4], which is very close to the presently found value. In addition, it is close to the 0 K value of 118.5 ± 1.0 kcal/mol reported by Holmes and Lossing [3,6]. However, it must be stressed that the present as well as the earlier Holmes and Lossing values are based on the nonexperimental value for the heat of formation of neutral methyl butanoate. On the other hand, the methyl acetate enol ion heat of formation derived from the TPEPICO data on the methyl acetate ion [4] is based on an experimental heat of formation of the methyl acetate molecule.

Finally, the adiabatic IE of the methyl butanoate was obtained by plotting the normalized molecular ion peak area versus photon energy near the ionization threshold. The onset energy was determined to be 9.95 ± 0.05 eV, giving $\Delta H^\circ_{f(0\ K)}$ of the methyl butanoate ion of 129 ± 1 kcal/mol (based on the

estimated heat of formation of the neutral methyl butanoate). The only literature IE value is 10.07 eV reported in 1962 by Watanabe [10]. This IE is extremely difficult to determine because of the significant change in the geometry of the molecule upon ionization. Since the barrier for isomerization is only about 1 kcal/mol, the ground state of the ion has a geometry that is apparently very much affected by the distonic ion well. Thus, the ion yield curve is very slowly rising in the vicinity of the onset and its precise location remains uncertain.

The RRKM modeling of the experimental results combined with our IE measurements shows that the distonic ion $CH_2CH_2CH_2COHOCH_3^{+}$ lies 9.5 kcal/mol below the methyl butanoate ion. Our ab initio MO calculations predicted that the distonic isomer B is 15.6 kcal more stable than the ionized methyl butanoate, which is 6 kcal/mol higher. However, this comparison depends upon the choice of ionization energies. If we choose the larger Watanabe value of 10.07 eV [10], the difference drops to about 3 kcal/mol. Either way, the difference falls within the error limit expected for the MP2(FULL)/6-31g* calculations.

5. Conclusion

The dissociation dynamics of methyl butanoate ions are well described by the simple mechanism A $\rightarrow$ B $\rightarrow$ $CH_2COHOCH_3^{+}$ + C_2H_4, in which A is the methyl butanoate ion, and B is a distonic isomer which resides in a well about 9.5–12.2 kcal/mol below that of the A isomer. The dissociation rate is single component and its rate is determined by the low energy B well. The product ion (the enol ion of methyl acetate) is produced via a simple bond fission. From the measured onset of 10.275 $\pm$ 0.010 eV, we derive a $\Delta H^{\circ}_{f(0K)}[CH_2COHOCH_3^{+}]$ of 122 $\pm$ 2 kcal/mol, whose uncertainty is determined by the estimated heat of formation of methyl butanoate. However, this value agrees well with a derived value from the analysis of the methyl acetate ion dissociation dynamics [4].

Acknowledgements

We would like to thank the Department of Energy for continuing financial support and the North Carolina Supercomputing facility for the generous allotment of computer time.

References

[1] T. Baer, O.A. Mazyar, J.W. Keister, P.M. Mayer, Ber. Bunsenges Phys. Chem. 101 (1997) 478.
[2] O.A. Mazyar, T. Baer, J. Phys. Chem. A 102 (1998) 1682.
[3] J.L. Holmes, F.P. Lossing, J. Am. Chem. Soc. 102 (1980) 1591.
[4] O.A. Mazyar, P.M. Mayer, T. Baer, Int. J. Mass Spectrom. Ion. Process. 167/168 (1997) 389.
[5] N. Heinrich, J. Schmidt, H. Schwarz, Y. Apeloig, J. Am. Chem. Soc. 109 (1987) 1317.
[6] J.L. Holmes, F.P. Lossing, Org. Mass Spectrom. 14 (1979) 512.
[7] K.M. Weitzel, J.A. Booze, T. Baer, Chem. Phys. 150 (1991) 263.
[8] T. Baer, W.B. Peatman, E.W. Schlag, Chem. Phys. Lett. 4 (1969) 243.
[9] R. Spohr, P.M. Guyon, W.A. Chupka, J. Berkowitz, Rev. Sci. Instrum. 42 (1971) 1872.
[10] K. Watanabe, T. Nakayama, J. Mottl, J. Quant. Spectrosc. Radiat. Transfer 2 (1962) 369.
[11] H. Schwarz, C. Wesdemiotis, Org. Mass. Spectrom. 14 (1979) 25.
[12] J.M.H. Pakarinen, P. Vainiotalo, C.L. Stumpf, D.T. Leeck, P.K. Chou, H.I. Kenttamaa, J. Am. Soc. Mass Spectrom. 7 (1996) 482.
[13] M.J. Frisch, G.W. Trucks, H.B. Schlegel, P.M.W. Gill, B.G. Johnson, M.A. Robb, J.R. Cheeseman, T. Keith, G.A. Petersson, J.A. Montgomery, K. Raghavachari, M.A. Al-Laham, V.G. Zakrzewski, J.V. Ortiz, J.B. Foresman, J. Cioslowski, B.B. Stefanov, A. Nanayakkara, M. Challacombe, C.Y. Peng, P.Y. Ayala, W. Chen, M.W. Wong, J.L. Andres, E.S. Replogle, R. Gomperts, R.L. Martin, D.J. Fox, J.S. Binkley, D.L. Defrees, J. Baker, J.P. Stewart, M. Head-Gordon, C. Gonzalez, J.P. Pople, GAUSSIAN 94, 1995.
[14] J.A. Pople, A.P. Scott, M.W. Wong, L. Radom, Isr. J. Chem. 33 (1993) 345.
[15] A.P. Scott, L. Radom, J. Phys. Chem. 100 (1996) 16 502.
[16] B.F. Yates, L. Radom, J. Am. Chem. Soc. 109 (1987) 2910.
[17] T. Baer, W.L. Hase, Unimolecular Reaction Dynamics: Theory and Experiments, Oxford, New York, 1996.
[18] J.W. Keister, P. Tomperi, T. Baer, Int. J. Mass Spectrom. Ion. Process. 171 (1997) 243.
[19] R.A. Marcus, O.K. Rice, J. Phys. Colloid Chem. 55 (1951) 894.
[20] H.M. Rosenstock, M.B. Wallenstein, A.L. Wahrhaftig, H. Eyring, Proc. Natl. Acad. Sci. 38 (1952) 667.

[21] D.G. Truhlar, B.C. Garrett, Acc. Chem. Res. 13 (1980) 440.
[22] W.L. Hase, J. Chem. Phys. 64 (1976) 2442.
[23] W.A. Chupka, J. Chem. Phys. 30 (1959) 191.
[24] C. Lifshitz, Mass Spectrom. Rev. 1 (1982) 309.
[25] S.G. Lias, et al., Gas Phase Ion and Neutral Thermochemistry, J. Phys. Chem. Ref. Data 17 (1988) (suppl 1).
[26] PCMODEL for Windows™ (Serena Software, Bloomington, IN, 1994). The MMX force field is an extension of N.L. Allinger's MM2 (QCPE-395, 1977) force field and includes pi routines from his MMP1 (QCPE-318). These are available from the Quantum Chemistry Program Exchange, Creative Arts Building 181, 840 State Highway 46 Bypass, Bloomington, IN 47405, Programs 395 and 318. Change were made by J.J. Gajewski and K.E. Gilbert, 1994.